Nonlinear Dynamics of Direction-selectivity in the Primary Visual Cortex

John R. Faust
The University of Utah Mathematics Department, The University of Utah, Salt Lake City, Utah 84112

The direction selectivity of cortical neurons can be accounted for by asymmetric lateral connections. Such lateral connectivity leads to network dynamics with characteristic properties that would distinguish this mechanism for direction selectivity from other possible mechanisms in neurophysiological experiments. This paper presents a mathematical analysis of a nonlinear model of direction-selective neurons with asymmetric lateral connections. The result of the analysis is that asymmetrically coupled networks can stabilize stimulus-locked traveling pulse solutions that are appropriate for the modeling of the responses of direction-selective neurons. Outside a certain regime of stimulus speeds the stability of these solutions breaks down, and under certain parameters, gives rise to lurching activity waves with specific spatiotemporal periodicity. Under other parameters other behaviors have been observed. Only lurching waves are discussed in this paper; the other behaviors are the subject of future research.

I. INTRODUCTION

While most models of direction selectivity employ feedforward mechanisms, the existence of strong lateral connectivity among cortical neurons motivates a model employing recurrent neural networks with asymmetric lateral excitatory or inhibitory connections to account for the properties of direction selective of cortical neurons. It should be stated that the relative contribution of feedforward and recurrent connectivity to the direction selectivity of cortical neurons remains an unresolved issue.

This paper presents a mathematical analysis of the nonlinear dynamics that arise in simple nonlinear neural networks with asymmetric recurrent connections driven by moving input stimuli. The result is that such networks have a class of form-stable solutions, stimulus-locked traveling pulses. The amplitude of these stable traveling pulse solutions depends on the stimulus velocity because of the asymmetric recurrent interactions in the network and are, therefore, suitable for modeling the activity of direction-selective neurons in the Primary Visual Cortex. Outside a certain regime of stimulus speed, the stability of the traveling pulse solutions breaks down and another class of solutions arises, lurching activity pulses. The bifurcation that underlies the transition between form-stable and lurching wave solutions results from the essentially nonlinear properties of the network dynamics. The existence of lurching activity pulses provides an experimentally testable prediction that is very specific for the explanation of direction selectivity by asymmetric lateral connections.

II. BASIC MODEL

A continuous approximation of the spatially discrete neuronal dynamics of the Primary Visual Cortex is

$$\textbf{(1)} \quad \tau\, \partial u(x,t)/\partial t = -u(x,t) + \int_\Omega w(x-x')\, f(u(x',t))\, dx' + b(x,t).$$

Where: u(x,t) is the scalar neural activity distribution characterizing the average activity at time t of an ensemble of functionally similar neurons that code for stimulus feature x;

w(x−x′) is interaction kernel characterizing the average synaptic connection strength between the neurons coding position x′ and the neurons coding position x. For section A. the only restriction for the interaction kernel is that it should allow for solutions with a single excited regime. In section B. an explicit interaction function will be defined and used.

f is the nonlinear activation function of the neurons

b(x,t) is the stimulus.

The two rightmost terms on the right hand side of the equation are the total input which includes a feedforward input term (b(x,t)) and a feedback term that integrates the recurrent contributions from other laterally connected neurons. This model uses dynamic neural fields to model the average behavior of a large ensemble of neurons.

In the presence of a stimulus with a constant activity profile that moves at a constant velocity υ, the mathematical description of the dynamics can be simplified by using a moving frame of coordinates by changing the spatial variable to $\xi = x - \upsilon t$. In this new frame the stimulus is stationary: $B(\xi) = b(x,t)$ and $U(\xi,t) = u(x,t)$ is the activity. By the Chain Rule, $\tau\, \partial u(x,t)/\partial t = \tau\, \partial U(\xi,t)/\partial t - \tau v\, \partial U(\xi,t)/\partial \xi$, and the dynamics become

$$\textbf{(2)} \quad \tau\, \partial U(\xi,t)/\partial t - \tau v\, \partial U(\xi,t)/\partial \xi = -U(\xi,t) + \int_\Omega w(\xi-\xi')\, f(U(\xi',t))\, d\xi' + B(\xi).$$

For a stationary solution in the moving frame $\partial U(\xi,t)/\partial t = 0$, so a stationary solution must satisfy

$$\textbf{(3)} \quad -\tau v\, \partial U^*(\xi)/\partial \xi = -U^*(\xi) + \int_\Omega w(\xi-\xi')\, f(U^*(\xi'))\, d\xi' + B(\xi).$$

The traveling pulse solution driven by the moving stimulus can be found by solving (3). The stability of the traveling pulse can be studied by perturbing the stationary solution in (2).

In most cases an analytical solution of these equations is impossible due to nonlinearity. However, for the biologically inspired step function, an analytical solution can be found.

III. STEP ACTIVATION FUNCTION

For the step activation function, $f(z) = 1$ when $z > 0$ and zero otherwise. This form of activation function approximates the activities of neurons that, by saturation, are either active or inactive.

Consider a one-dimensional neural field and assume that only a single stationary excited regime with $[U^*(\xi) > 0]$ exists and is located between the points (ξ^*_1, ξ^*_2). Only neurons inside this regime contribute to the integral. Because f is constant in this regime, this contribution only depends on the boundary values ξ^*_1 and ξ^*_2.

With the function W(x) satisfying W'(x) = w(x), the spatial shape of $U^*(\xi)$ of the stationary solution obeys the ordinary differential equation,

$$(4) \quad -\tau v\, \partial U^*(\xi)/\partial\xi = -U^*(\xi) + W(\xi-\xi^*_1) - W(\xi-\xi^*_2) + B(\xi).$$

Treating the boundaries ξ^*_1 and ξ^*_2 as fixed parameters the solution of this equation can be found. To facilitate notation let the integral operator O with parameter $\alpha \neq 0$ be $O[g(z);\alpha] \equiv \int_{zo}^{z} g(m)\, e^{(z-m)/\alpha}\, dm$, where $zo = -\infty$ for $\alpha < 0$ and $zo = +\infty$ for $\alpha > 0$. Define two function $F(z) = O[W(z);\tau\upsilon]/(-\tau\upsilon)$ and $G(z) = O[B(z);\tau\upsilon]/(-\tau\upsilon)$. The solution to (4) can be written with these two functions as

$$(5) \quad U^*(\xi) = F(\xi-\xi^*_1) - F(\xi-\xi^*_2) + G(\xi).$$

For the boundary points, $U^*(\xi_1^*) = U^*(\xi_2^*) = 0$ must be satisfied, leading to the transcendental equations system,

$$(6) \quad -F(0) + F(\xi_1^*-\xi_2^*) = G(\xi_1^*),$$

$$(7) \quad F(0) - F(\xi_2^*-\xi_1^*) = G(\xi_2^*),$$

from which ξ_1^*, ξ_2^* can be determined. To be consistent with initial assumption, it has to be verified that the solutions $U^*(\xi)$ has only one excited regime between ξ_1^*, ξ_2^*.

A. Stability of the traveling pulse solution

The stability of the traveling pulse solutions can be analyzed by perturbing the dynamics around the stationary solution in the moving frame. In this analysis of this section, the only restriction for the interaction kernel is that it allows for solutions with a single excited regime. To give consideration to the step threshold nonlinearity in the dynamics, both the wave form and the boundary points are perturbed. Also, the perturbation of the boundary points can be related to the perturbation of the wave form at the boundary points. Based on this, the eigenvalue equation for the linearized perturbation dynamics are

$$(9) \quad [\, K(0) - c_i^*(1+\tau\lambda)\,]\,[\, K(0) + c_2^*(1+\tau\lambda)\,] = K(\xi_1^*-\xi_2^*)\, K(\xi_2^*-\xi_1^*),$$

where $c_i^* \equiv dU^*(\xi_i)/d\xi$ for i =1, 2, and the function K(z) defined as $K(z) \equiv O[w(z);\tau\upsilon/(1+\tau\lambda)](1+\tau\lambda)/(-\tau\upsilon)$. From (9) the eigenvalues (λ) can be found numerically. The traveling pulse solution is asymptotically stable only if the real parts of all eigenvalues that solve (9) are nonpositive. The eigenvalue equation is derived in detail in the next section on stability analysis.

1. Stability analysis

The stability of the traveling pulse solution is analyzed by perturbing the stationary solution in the moving coordinate system. Let $\delta U(\xi,t)$ be a small perturbation of $U^*(\xi)$. The linearized perturbation dynamics reads

$$\tau\, \partial(\delta U)/\partial t - \tau\upsilon\, \partial(\delta U)/\partial\xi + \delta U(\xi,t) = -\delta\xi_1\, w(\xi-\xi_1^*) + \delta\xi_2\, w(\xi-\xi_2^*), \quad \textbf{(10)}$$

where $\delta\xi_i$ for i =1, 2 are the perturbations of the boundary points of the excited regime from the stationary values of ξ_i^* with $\xi_i = \xi_i^* + \delta\xi_i$ satisfying $U(\xi_i,t) = 0$. Note that $\delta\xi_i$ is not independent of $\delta U(\xi,t)$, and the dependence can be found through

$$U(\xi_i^*+\delta\xi_i\ ,t) = U(\xi_i^*,t) + \delta\xi_i\ \partial U(\xi_i^*,t)/\partial\xi + O(\delta\xi_i^2) = 0. \quad \textbf{(11)}$$

Since $U(\xi_i^*,t) = \delta U(\xi_i^*,t)$ to the first order, $\delta\xi_i = -\delta U(\xi_i^*,t)/c_i^*$, where $c_i^* \equiv dU^*(\xi_i)/d\xi$. Substituting this back into the perturbed dynamics, the perturbed dynamics with perturbations in U only are derived as

$$\tau\, \partial(\delta U)/\partial t - \tau\upsilon\, \partial(\delta U)/\partial\xi + \delta U(\xi,t) = \delta U(\xi_1^*,t)\, w(\xi-\xi_1^*)/c_1^* - \delta U(\xi_2^*,t)\, w(\xi-\xi_2^*)/c_2^*. \quad \textbf{(12)}$$

The stability of (12) can be checked by the time-honored method of wild-guessing, also known as the more respectable sounding German "ansatz" method of substituting a solution of the form $\delta U(\xi,t) = e^{\lambda t}\, Y(\xi)$ into (12) and deriving the equation for $Y(\xi)$:

$$-\tau\upsilon\, Y'(\xi) + (1 + \tau\lambda)\, Y(\xi) = Y(\xi_1^*)\, w(\xi-\xi_1^*)/c_1^* - Y(\xi_2^*)\, w(\xi-\xi_2^*)/c_2^*. \quad \textbf{(13)}$$

(13) can be solved by first assuming that $Y(\xi_1^*)$ and $Y(\xi_2^*)$ are constant, and afterwards giving self-consistent conditions for the solutions at ξ_1^* and ξ_2^* to satisfy. The solution of (13) is then

$$Y(\xi) = Y(\xi_1^*)\, K(\xi-\xi_1^*)/(\, c_1^*(1+\tau\lambda)\,) - Y(\xi_2^*)\, K(\xi-\xi_2^*)/(\, c_2^*(1+\tau\lambda)\,), \quad \textbf{(14)}$$

for which the self-consistent conditions for the solutions at ξ_1^* and ξ_2^* are

$$Y(\xi_1^*) = Y(\xi_1^*)\, K(0)/(\, c_1^*(1+\tau\lambda)\,) - Y(\xi_2^*)\, K(\xi_1^*-\xi_2^*)/(\, c_2^*(1+\tau\lambda)\,), \quad \textbf{(15)}$$

$$Y(\xi_2^*) = Y(\xi_1^*)\, K(\xi_2^*-\xi_1^*)/(\, c_1^*(1+\tau\lambda)\,) - Y(\xi_2^*)\, K(0)/(\, c_2^*(1+\tau\lambda)\,). \quad \textbf{(16)}$$

For (15) and (16) to have a solution, (9) has to be satisfied.

B. Simulation results of the step activation function model

The mathematical results of section A. can be tested by numerically simulating the model using an interaction function ($w(x-x')$) given by a difference of two exponential functions:

$$w(x) = a_e \exp(\, -k_e\, |x-x_o|\,) - a_i \exp(-k_i\, |x-x_o|\,), \quad \textbf{(17)}$$

where a_e and a_i are the amplitudes of excitation and inhibition and x_o is an offset that causes the network to be asymmetric and induces the direction sensitivity. This function simulates a receptive field with asymmetric local excitation and center-surround inhibition. The advantage of using exponentials is that the integration of the integral operator O can be carried out explicitly, which simplifies subsequent calculations considerably. Also for the numerical simulation, the stimulus, b(x,t), is a moving bar with constant width and amplitude.

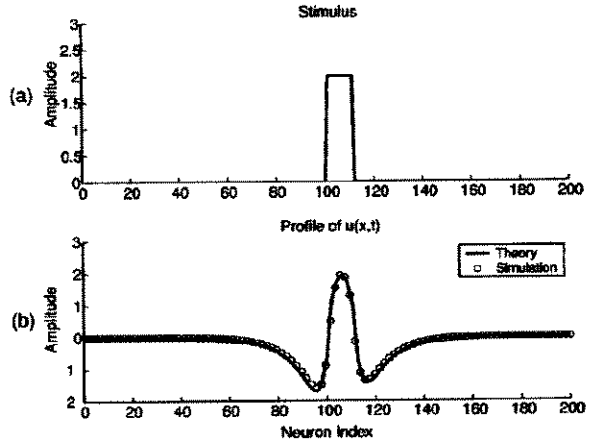

FIG. 1. Stimulus and activity profile in the step activation function model. Panel (a) shows the stimulus, and panel (b) the activity $m(x,t)$ at the time t for the traveling pulse solution. The solid line in (b) shows the result from the calculation, while the circles indicate the numerical simulation results. The interaction kernel used in this simulation was $w(x)=a_e\exp(-k_e|x-x_0|)-a_i\exp(-k_i|x-x_0|)$ with $a_e=1$, $a_i=5$, $k_e=0.42$, $k_i=0.1$, and $x_0=3$. The stimulus was a moving bar with width $d=10$ and amplitude $h=2$. Notice that the activity profile $u(x,t)$ has only a single excited regime.

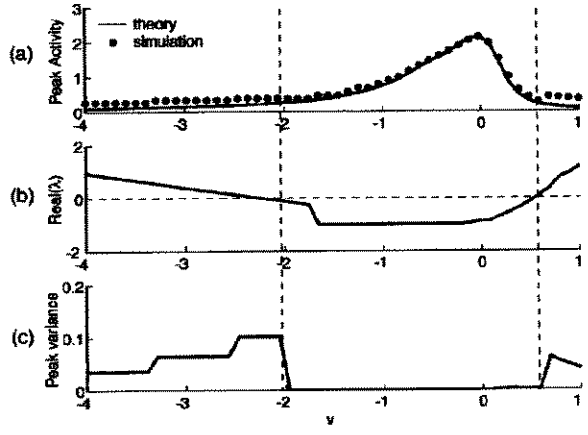

FIG. 2. Traveling pulse solution and its stability in the step activation function model. Panel (a) shows the velocity tuning curves and the peak amplitude of the traveling pulse. The solid lines indicate the theoretical results, while the dots signify the numerical simulation results. The velocity v is normalized by the time constant of the dynamics in the unit of rad/τ. Panel (b) shows the largest real parts of the eigenvalue λ obtained by solving Eq. (9) numerically. Only solutions corresponding to the negative values of this function are form stable. Panel (c) plots the variations of the peak amplitude of the pulse. A variance that deviates significantly from zero signifies a loss of stability of the traveling pulse solutions. The results are consistent with analysis of the eigenvalues in panel (b). Also notice that in panel (a) the theoretical peak amplitude fits well the simulation results only inside the stable regime.

Figure 1 plots a snapshot of the activity profile of u(x,t) and stimulus b(x,t) at a time t in the regime where the traveling pulse solution is stable. The simulation results are plotted on top of the analytically calculated profile u(x,t), and are consistent with the theory. A typo occurred in Fig. 1; a_e should be 5 and a_i should be 1, with a_e=1 and a_i=5, the weight function is not a Mexican-hat.

Figure 2 shows the peak activity of u(x,t) as a function of the stimulus speed. Panel (a) shows the speed tuning curve plotted as the dependence of the peak activity of the traveling pulse as a function of the stimulus velocity v. The solid line indicates the results from the theoretical solution and the dots indicate the simulation results. Panel (b) shows the maximum of the real parts of the eigenvalues obtained from (9). For stimulus velocity

outside a certain range, this maximum becomes positive indicating a loss of stability of the form-stable solution. To verify this result the variability of the peak activity over time can be calculated after excluding the initial transients from the simulations. Panel (c) shows the variations as a function of the stimulus velocity. At the velocities for which the eigenvalues indicate a loss of stability, the variability of the amplitudes suddenly increases. This indicates that the stationary solution is not time independent any more, which is consistent with the interpretation that the form-stable solution loses stability.

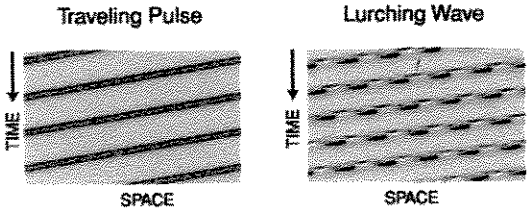

FIG. 3. Traveling pulse and lurching wave in step activation function model. The color-coded plots show the spatial-temporal evolution of the activity $u(x,t)$. The left panel shows the propagation of the form-stable peak over time. The right panel shows the lurching activity wave that arises when stability is lost.

Figure 3 shows the space-time evolution of the activity. The left panel shows the propagation of the form-stable traveling pulse for medium stimulus speeds. The right panel shows the solution that arises when stability is lost. This "lurching wave" solution is characterized by spatiotemporal periodicity that is defined in the moving coordinate system by $U(y + mL_o, t + nT_o) = U(y,t)$, where L_o and T_o are constants that depend on the network dynamics. These solutions are termed lurching waves because of the periodic discontinuity of the spatiotemporal evolution of the neural activity. Lurching wave activity also arises in this type of network for other forms of interaction kernels or input signals as well as for other types of threshold functions [1].

IV. CONCLUSIONS

This paper has presented a mathematical analysis of a class of models that account for direction selectivity by asymmetric lateral connections between cortical neurons. Given the large number of recurrent connections in the visual cortex, it is plausible that lateral connections play an important role for the realization of direction selectivity [2,3]. The proposed recurrent mechanism for direction selectivity exploits a kind of "resonance" between the tendency of the network to stabilize a traveling pulse solution with characteristic speed and the incoming time-dependent stimulus activity.

One result of this analysis is that such recurrent models, for a certain regime of stimulus speeds, have traveling pulse solutions that are form stable and move with the same speed as the stimulus. Such solutions are termed stimulus-locked traveling pulses. In the stationary case, these solutions have space-time characteristics that are also compatible with other models for direction selectivity, e.g., motion energy models with feedforward structure, or models with linear feedback [1]. In particular, the recurrent mechanism analyzed in this model can account for biologically realistic degrees of velocity tuning in cortical neurons [4]. The preferred speed of the neurons in such recurrent models is determined by the network structure. Speed tuning analyzed in this nonlinear model arises because, for sufficiently strong interaction, the network tends to stabilize a traveling peak solution that "locks" to the moving activity peak of the stimulus. For the stimulus-locked traveling pulse solution the propagation speed is given by the stimulus. This solution becomes unstable if this locking is lost.

The stability analysis shows that the traveling pulse solution is stable only within a certain regime of stimulus speeds. At the borders of this regime a Hopf bifurcation arises and the stimulus-locked solution becomes unstable. Such speed-dependent bifurcations cannot arise in the classical feedforward models or in networks with linear feedback. For such networks the solutions are either always stable or the network is unstable [1].

One result of the simulation is that the loss of stability of the stimulus-locked solution is frequently accompanied by the formation of lurching activity pulses. Lurching activity has been described in brain slice experiments [5,6] and in studies with artificial spiking networks without time-dependent input signals [7,8]. The simulation results imply that spiking neurons are not necessary for the generation of lurching activity waves if a moving stimulus is present. Such lurching waves cannot be produced by a feedforward network, in which the output of the network is always phase locked to the stimulus. Moreover, there is no stability issue in feedforward networks. Therefore, the bifurcation observed in recurrent networks cannot appear in feedforward networks making these solutions difficult to accounted for by classical models of direction selectivity.

A final conclusion from the analysis is that the observation of lurching activity waves in populations of direction-selective neurons in the visual cortex would be a strong indicator for the relevance of the recurrent mechanism for direction selectivity discussed in this paper. Lurching waves and the related Hopf bifurcations might be experimentally observable by the recording from populations of direction selective neurons.

A note on future research. This paper, like the paper by X. Xie and M. A. Giese [1] it has followed, only discusses the breakdown of the stable stimulus-locked traveling pulses into unstable lurching waves. However, Dr. Xie and Dr. Giese's paper is incomplete. The network dynamics are much richer than presented in their paper. When the simulations were run under different parameters than those of Dr. Xie and Dr. Giese's paper, the stable pulse was observed to breakdown into unstable waves very different from the lurching wave. Besides becoming a lurching wave, the stable pulse was seen to permanently excite periodic areas of cortex. This created dynamics that seem to be somewhere between a stable pulse and a lurching wave, where there was simultaneously a stable pulse and lurches between stationary areas of excitation. The behavior of these and other unstable solutions and the conditions under which they arise are the next step in my research and will hopefully give a complete analysis of the nonlinear dynamics of direction-selectivity in the primary visual cortex.

ACKNOWLEDGEMENTS

None of this work would have taken place or made any sense to me with out Dr. Paul Bressloff, my mentor during this last year. Everything I know about numerical simulations I owe to the soon to be Dr. Stefan Folias. The push to finally pursue mathematical research came from Dr. Anne Roberts. Dr. Fred Adler and Dr. Elena Cherkaev, my Mathematical Biology and Nonlinear Dynamics and Chaos professors, respectively, have helped keep the place of this work in focus. Dr. Adler also has taught me the value of the German language in legitimizing strange mathematical practices. To all much thanks.

REFERENCES

[1] X. Xie and M. A. Giese, Phys. Rev. E. **65**, 051904 (2002).

[2] H. Suarez, C. Koch, and R. Douglas, J. Neurosci. **15**, 6700 (1995).

[3] R. Maex and G. A. Orban, J. Neuophysiol. **75**, 1515 (1996).

[4] P. Mineiro and D. Zipser, Neural Comput. **10**, 353 (1998).

[5] M. von Krosigk, T. Bal, and D. A. McCormick, Science **261**, 361 (1993).

[6] T. Bal, M. von Krosigk, and D. A. McCormick, J. Physiol. (London) **261**, 641 (1995).

[7] D. Golomb and G. B. Ermentrout, Proc. Natl. Aca. Sci. U.S.A. **96**, 13480 (1999).

[8] D. Golomb and G. B. Ermentrout, Phys. Rev. Lett. **86**, 4179 (2001).